

# ROSAT observations of warm absorbers in AGN

Stefanie Komossa, Henner Fink

Max-Planck-Institut für extraterrestrische Physik, 85740 Garching, Germany

## Abstract:

We study the properties of warm absorbers in several active galaxies (AGN) and present new candidates, using *ROSAT* X-ray observations. Several aspects of the characteristics of warm absorbers are discussed: (i) constraints on the density and location of the ionized material are provided; (ii) the impact of the presence of the warm gas on other observable spectral regions is investigated, particularly with respect to the possibility of a warm-absorber origin of one of the known high-ionization emission-line region in AGN; (iii) the possibility of dust mixed with the warm material is critically assessed; and (iv) the thermal stability of the ionized gas is examined. Based on the properties of known warm absorbers, we then address the question of where else ionized absorbers might play a role in determining the traits of a class of objects or individual peculiar objects. In this context, the possibility to produce the steep soft X-ray spectra of narrow-line Seyfert-1 galaxies by warm absorption is explored, as compared to the alternative of an accretion-produced soft excess. The potentiality of explaining the strong spectral variability in RX J0134-42 and the drastic flux variability in NGC 5905 via warm absorption is scrutinized.

## 1 Introduction and motivation

Absorption edges have been found in the X-ray spectra of several Seyfert galaxies and are interpreted as the signature of ionized gas along the line of sight to the active nucleus. This material, the so-called ‘warm absorber’, provides an important new diagnostic of the AGN central region, and hitherto revealed its existence mainly in the soft X-ray spectral region. The nature, physical state, and location of this ionized material, and its relation to other nuclear components, is still rather unclear. E.g., an outflowing accretion disk wind, or a high-density component of the inner broad line region (BLR) have been suggested.

The presence of an ionized absorber was first discovered in *Einstein* observations of the quasar MR 2251-178 (Halpern 1984). With the availability of high quality soft X-ray spectra from *ROSAT* and *ASCA*, several more warm absorbers were found: they are seen in about 50% of the well studied Seyfert galaxies (e.g. Nandra & Pounds 1992, Turner et al. 1993, Mihara et al. 1994, Weaver et al. 1994, Cappi et al. 1996) as well as in some quasars (e.g. Fiore et al. 1993, Ulrich-Demoulin & Molendi 1996, Schartel et al. 1997). More than one warm absorber imprints its presence on the soft X-ray spectrum of MCG-6-30-15 (Fabian 1996, Otani et al. 1996) and NGC 3516 (Kriss et al. 1996). Evidence for an influence of the ionized material on non-X-ray parts of the spectrum is

still rare: Mathur and collaborators (e.g. Mathur et al. 1994) combined UV and X-ray observations of some AGN to show the X-ray and UV absorber to be the *same* component. Emission from  $\text{NeVIII}\lambda 774$ , that may originate from a warm absorber, was discovered in several high-redshift quasars (Hamann et al. 1995).

The warm material is thought to be photoionized by emission from the central continuum source in the active nucleus. Its degree of ionization is higher than that of the bulk of the BLR and the gas temperature is typically of order  $10^5$  K. The properties of hot photoionized gas were studied e.g. in Krolik & Kallman (1984), Netzer (1993), Krolik & Kriss (1995), and Reynolds & Fabian (1995).

Here we analyze the X-ray spectra of several Seyfert galaxies, using *ROSAT* PSPC observations that nicely trace the spectral region in which the warm absorption features are located. In a first part, the properties of the ‘safely’ identified warm absorbers in the Seyfert galaxies NGC 4051, NGC 3227, and Mrk 1298 are derived, as far as X-ray spectral fits allow. These absorbers span a wide range in ionization parameter. Their properties are then further discussed in light of the known multi-wavelength characteristics of the individual Seyfert galaxies. E.g., the optical spectra show several features that may be directly (high-ionization emission lines, strong reddening), or indirectly (FeII complexes) linked to the presence of the warm absorber. In a second part, we will assess whether some properties of other classes of objects or individuals can be understood in terms of warm absorption. In particular, the existence of objects with *deeper* absorption complexes that recover only beyond the *ROSAT* energy range is expected (unless an as yet unknown fine-tuning mechanism is at work, that regulates the optical depths in the important metal ions). In this line, it is examined whether the presence of a warm absorber is a possible cause of the X-ray spectral steepness in narrow-line Seyfert 1 (NLSy1) galaxies. Furthermore, we scrutinize whether the strong spectral variability in RX J0134-42, and the drastic flux variability in NGC 5905 can be traced back to the influence of a warm absorber.

## 2 Models

The warm material was modeled using the photoionization code *Cloudy* (Ferland 1993). We assume the absorber (i) to be photoionized by continuum emission of the central pointlike nucleus, (ii) to be homogeneous, (iii) to have solar abundances (Grevesse & Anders 1989), and (iv) in those models that include dust mixed with the warm gas, the dust properties are like those of the Galactic interstellar medium, and the abundances are depleted correspondingly (Ferland 1993).

The ionization state of the warm absorber can be characterized by the hydrogen column density  $N_w$  of the ionized material and the ionization parameter  $U$ , defined as

$$U = Q/(4\pi r^2 n_{\text{H}}) \quad (1)$$

where  $Q$  is the number rate of incident photons above the Lyman limit,  $r$  is the distance between central source and warm absorber,  $n_{\text{H}}$  is the hydrogen

density (fixed to  $10^{9.5} \text{ cm}^{-3}$  unless noted otherwise) and  $c$  the speed of light. Both quantities,  $N_w$  and  $U$ , are determined from the X-ray spectral fits.

The spectral energy distribution (SED) chosen for the modeling corresponds to the observed multi-wavelength continuum in case of NGC 4051 and two of the NLSy1s, a mean Seyfert continuum with energy index  $\alpha_{\text{uv}-x} = -1.4$  else. The influence of the non-X-ray parts of the continuum shape will be commented on in Sect. 3.1, which will show the assumption of a mean Seyfert SED to be justified. However, the EUV part of the SED contributes to the numerical value of  $U$ . For better comparison of the ionization states of the discussed warm absorbers, we also give the quantity  $\tilde{U}$  for each object, which is  $U$  normalized to the mean Seyfert continuum with  $\alpha_{\text{uv}-x} = -1.4$ .

The X-ray data reduction was performed in a standard manner, using the EXSAS software package (Zimmermann et al. 1994).

### 3 NGC 4051

NGC 4051 is a low-luminosity Seyfert galaxy with a redshift of  $z=0.0023$ , classified as Seyfert 1.8 or NLSy1. It is well known for its rapid X-ray variability and has been observed by all major X-ray missions. Evidence for the presence of a warm absorber was discovered by Pounds et al. (1994) in the *ROSAT* survey observation. We have analyzed all archival observations of NGC 4051 (part of those were independently presented by McHardy et al., 1995) and PI data taken in Nov. 1993. Emphasis is put on the latter observation, and the results refer to these data if not stated otherwise (for details on the Nov. 93 observation see Komossa & Fink 1997; for the earlier ones Komossa & Fink 1996).

#### 3.1 Spectral analysis

A single powerlaw gives a poor fit to the X-ray spectrum of NGC 4051 ( $\chi^2_{\text{red}} = 3.8$ ) and the resulting slope is rather steep (photon index  $\Gamma_x = -2.9$ ). A warm absorber model describes the spectrum well, with an ionization parameter of  $\log U = 0.4$  ( $\log \tilde{U} = 0.8$ ), a large warm column density of  $\log N_w = 22.67$ , and an intrinsic powerlaw spectrum with index  $\Gamma_x = -2.3$ . The unabsorbed (0.1-2.4 keV) luminosity is  $L_x = 9.5 \times 10^{41} \text{ erg/s}$  (for a distance of 14 Mpc). The addition of the absorber-intrinsic emission and far-side reflection to the X-ray spectrum, calculated for a covering factor of the warm material of 0.5, only negligibly changes the results ( $\log N_w = 22.70$ ) due to the weakness of these components.

We note, that the intrinsic, i.e. unabsorbed, powerlaw with index  $\Gamma_x = -2.3$  is steeper than the Seyfert-1 typical value with  $\Gamma_x = -1.9$  and it is also in its steepest observed state in NGC 4051. We have verified that no additional soft excess causes an apparent deviation from the canonical index, although the presence of such a component, with  $kT_{\text{bb}} \simeq 0.1 \text{ keV}$ , is found in the high-state data.

The observed multi-wavelength SED for NGC 4051 was used for the above analysis, with  $\alpha_{\text{uv}-x} = -0.7$ . In some further model sequences, the influence of the

continuum shape on the results was tested, by (i) the addition of an EUV black body component with variable temperature and normalization (chosen such that there is no contribution of that component to the observed UV or X-ray part of the spectrum), and (ii) the inclusion of a strong IR spectral component as observed by IRAS (although at least part of it is most probably due to emission by cold dust from the surrounding galaxy; e.g. Ward et al. 1987). We find: (i) an additional black body component in the EUV has negligible influence on the X-ray absorption structure; (ii) an additional IR component strongly increases the free-free heating of the gas and the electron temperature rises. The best-fit ionization parameter changes to  $\log U = 0.2$ .

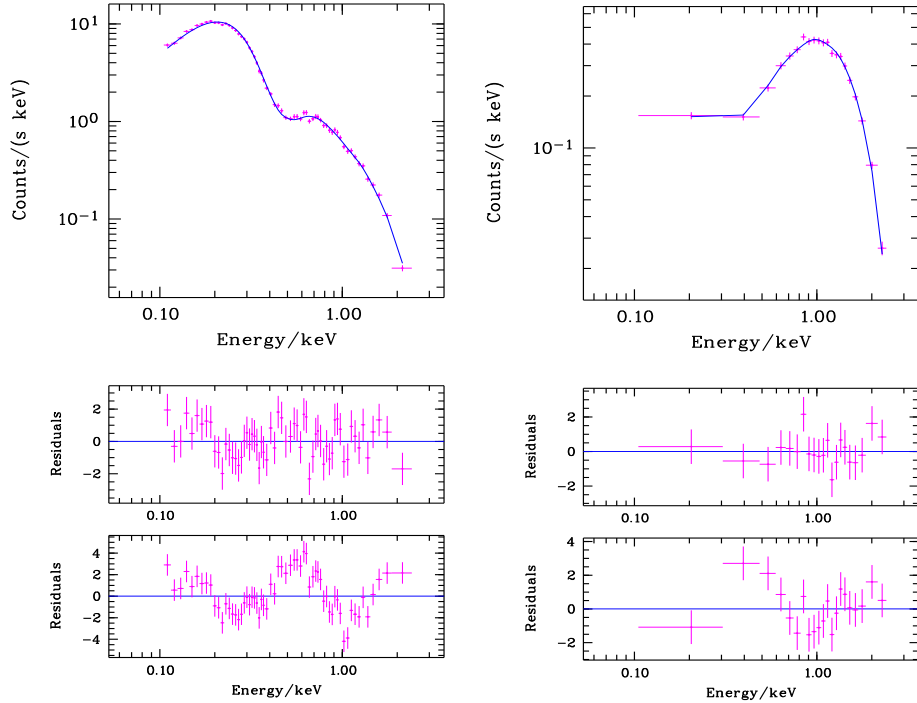


**Fig. 1.** Left: The upper panel shows the observed X-ray spectrum of NGC 4051 (crosses) and the best-fit warm absorber model (solid line). The next panel displays the fit residuals for this model. For comparison, the residuals resulting from a single powerlaw description of the data are shown in the lower panel (note the different scale in the ordinate). Right: The same for NGC 3227.

### 3.2 Temporal analysis

We detect strong variability: The largest amplitude is a factor of  $\sim 30$  in count rate during the 2 year period of observations. In the Nov. 1993 observation, NGC 4051 is variable by about a factor of 6 within a day. The amplitude of variability is essentially the same in the low energy ( $E \leq 0.5$  keV; dominated by the cold-absorbed powerlaw) and high energy (dominated by ionized-absorption) region of the *ROSAT* band (Fig. 2). To check for variability of the absorption edges in more detail, we have performed spectral fits to individual subsets of the total observation (referred to as ‘orbits’ hereafter). The best-fit ionization parameter turns out to be essentially constant over the whole observation despite strong changes in intrinsic luminosity. This constrains the, a priori unknown, density and hence location of the warm absorber (see below).

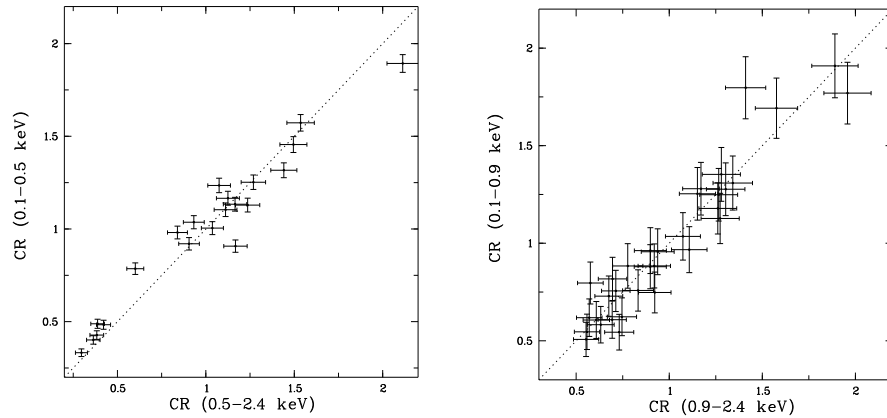


**Fig. 2.** Count rate CR in the soft *ROSAT* energy band versus count rate in the hard band, each normalized to the mean count rate in the corresponding band. Left: NGC 4051, right: NGC 3227. The dotted line represents a linear correlation.

### 3.3 Properties of the warm absorber

**Density** A limit on the density  $n$  can be drawn from the spectral (non-)variability, i.e. the constancy of  $U$  during a factor of  $> 4$  change in intrinsic luminosity. The reaction timescale  $t_{\text{rec}}$  of the ionized material is conservatively estimated from the lack of any reaction of the warm material during the long low-state in orbit 7, resulting in a recombination timescale  $t_{\text{rec}} \gtrsim 2000$  s. The upper limit on the density is given by

$$n_e \approx \frac{1}{t_{\text{rec}}} \frac{n_i}{n_{i+1}} \frac{1}{A} \left( \frac{T}{10^4} \right)^X \quad (2)$$

where  $n_i/n_{i+1}$  is the ion abundance ratio of the dominant coolant and the last term is the corresponding recombination rate coefficient  $\alpha_{i+1,i}^{-1}$  (Shull & Van

Steenberg 1982). We find  $n \lesssim 3 \times 10^7 \text{ cm}^{-3}$ , dismissing a high-density BLR component as possible identification of the warm absorber that dominates the Nov. 93 spectrum. The corresponding thickness of the ionized material is  $D \gtrsim 2 \times 10^{15} \text{ cm}$ .

**Location** The location of the warm material is poorly constrained from X-ray spectral fits alone. Using  $Q = 1.6 \times 10^{52} \text{ s}^{-1}$  and the upper limit on the density, yields a distance of the absorber from the central power source of  $r \gtrsim 3 \times 10^{16} \text{ cm}$ . Conclusive results for the distance of the BLR in NGC 4051 from reverberation mapping, that would allow a judgement of the position of the warm absorber relative to the BLR, do not yet exist: Rosenblatt et al. (1992) find the continuum to be variable with high amplitude, but no significant change in the  $\text{H}\beta$  flux.

**Warm-absorber intrinsic line emission and covering factor** For 100% covering of the warm material, the absorber-intrinsic  $\text{H}\beta$  emission is only about 1/220 of the observed  $L_{\text{H}\beta}$ . The strongest optical emission line predicted to arise from the ionized material is  $[\text{FeXIV}]\lambda 5303$ . Its scaled intensity is  $[\text{FeXIV}]_{\text{wa}}/\text{H}\beta_{\text{obs}} \approx 0.01$ . This compares to the observed upper limit of  $[\text{FeXIV}]/\text{H}\beta \lesssim 0.1$  (Peterson et al. 1985) and it is consistent with a covering of the warm material of less or equal 100%. Due to the low emissivity of the warm gas in NGC 4051, no strong UV – EUV emission lines are produced (e.g.  $\text{HeII}\lambda 1640_{\text{wa}}/\text{H}\beta_{\text{obs}} \leq 0.06$ ,  $\text{NeVIII}\lambda 774_{\text{wa}}/\text{H}\beta_{\text{obs}} \leq 0.2$ ). Consequently, no known emission-line component in NGC 4051 can be fully identified with the warm absorber. We have verified that this result holds independently of the exact value of density chosen, as well as (IR or EUV) continuum shape.

**UV absorption lines** Due to the low column densities in the relevant ions, the predicted UV absorption lines are rather weak. The expected equivalent widths for the UV lines  $\text{CIV}\lambda 1549$ ,  $\text{NV}\lambda 1240$  and  $\text{Ly}\alpha$  are  $\log W_{\lambda}/\lambda \simeq -4.0$ ,  $\log W_{\lambda}/\lambda \simeq -4.7$ , and  $\log W_{\lambda}/\lambda \simeq -3.0$ , respectively (for a velocity parameter  $b = 60 \text{ km/s}$ ; Spitzer 1978).

**Influence of dust** Dust might be expected to survive in the warm absorber, depending on its distance from the central energy source and the gas-dust interactions. A dusty environment was originally suggested as an explanation for the small broad emission-line widths in NLSy1 galaxies. Warm material with internal dust was proposed to exist in the quasar IRAS 13349+2438 (Brandt et al. 1996). The evaporation distance  $r_{\text{ev}}$  of dust due to heating by the radiation field is provided by  $r_{\text{ev}} \approx \sqrt{L_{46}} \text{ pc}$  (e.g. Netzer 1990). For NGC 4051 we derive  $r_{\text{ev}} \approx 0.02 \text{ pc}$ .

Mixing dust of Galactic ISM properties (including both, graphite and astronomical silicate; Ferland 1993) with the warm gas in NGC 4051 and self-consistently re-calculating the models leads to maximum dust temperatures of 2200 K (graphite) and 3100 K (silicate), above the evaporation temperatures (for a density of  $n_{\text{H}} = 5 \times 10^7 \text{ cm}^{-3}$  and  $U$ ,  $N_{\text{w}}$  of the former best-fit model). For  $n_{\text{H}} \lesssim 10^6 \text{ cm}^{-3}$ , dust can survive throughout the absorber. However, it changes the equilibrium conditions and ionization structure of the gas. For relatively

high ionization parameters, dust very effectively competes with the gas in the absorption of photons (e.g. Netzer & Laor 1993).

Firstly, re-running a large number of models, we find no successful fit of the X-ray spectrum. This can be traced back to the relatively higher importance of edges from more lowly ionized species, and particularly a very strong carbon edge (Fig. 3). There are various possibilities to change the properties of dust mixed with the warm material. The one which weakens observable features, like the 2175 Å absorption and the  $10\mu$  IR silicon feature, and is UV gray, consists of a modified grain size distribution, with a dominance of larger grains (Laor & Draine 1993). However, again, such models do not fit the observed X-ray spectrum, even if silicate only is assumed to avoid a strong carbon feature and its abundance is depleted by 1/10.

The absence of dust in the warm material would imply either (i) the *history* of the warm gas is such that dust was never able to form, like in an inner-disc driven outflow (e.g. Murray et al. 1995, Witt et al. 1996) or (ii) if dust originally existed in the absorber, the *conditions* in the gas have to be such that dust is destroyed. In the latter case, one obtains an important constraint on the density (location) of the warm gas, which then has to be high enough (near enough) to ensure dust destruction. For the present case (and Galactic-ISM-like dust) only a narrow range in density around  $n_{\text{H}} \approx 5 \times 10^7 \text{ cm}^{-3}$  is allowed. For lower densities, dust can survive in at least part of the absorber and higher densities have already been excluded on the basis of variability arguments.

### 3.4 Evidence for an ‘EUV bump’

The warm absorber fit shown in Fig. 1 shows some residual structure between 0.1 and 0.3 keV that can be explained by an additional very soft excess component. Of course, the parameters of such a component are not well constrained from X-ray spectral fits. One with  $kT_{\text{bb}} = 13 \text{ eV}$  and an integrated absorption-corrected flux (between the Lyman limit and 2.4 keV) of  $F = 7 \times 10^{-11} \text{ erg/cm}^2/\text{s}$  fits the data. It contributes about the same amount to the ionizing luminosity as the powerlaw continuum used for the modeling and has the properties of the EUV spectral component for which evidence is as follows:

A lower limit on the number rate  $Q$  of ionizing photons in the unobserved EUV-part of the SED can be estimated by a powerlaw interpolation between the flux at 0.1 keV (from X-ray spectral fits) and the Lyman-limit (by extrapolating the observed UV spectrum), which was used for the present modeling. This gives  $Q = 1.6 \times 10^{52} \text{ s}^{-1}$ .

$Q$  can also be deduced from the observed  $\text{H}\beta$  luminosity. Both quantities are related via  $Q = (2.1 - 3.8) \times 10^{12} L_{\text{H}\beta}$  (Osterbrock 1989). The mean observed  $L_{\text{H}\beta} = 7.8 \times 10^{39} \text{ erg/s}$  (Rosenblatt et al. 1992) yields  $Q = (1.6 - 2.5) \times 10^{52} \text{ s}^{-1}$ . It is interesting to note that this is of the same order as the lower limit determined from the assumption of a single powerlaw EUV-SED, suggesting the existence of an additional EUV component in NGC 4051.

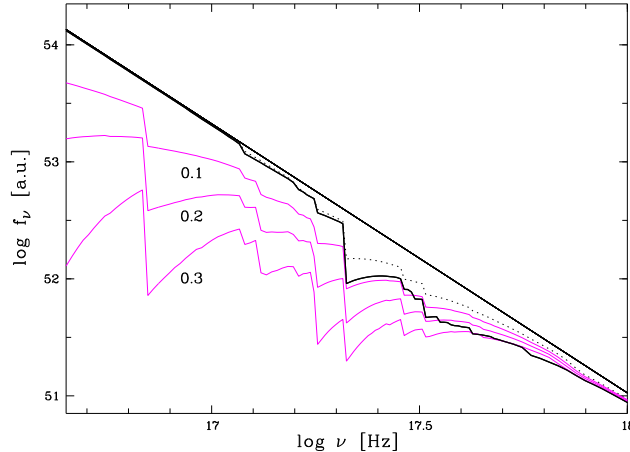


**Fig. 3.** Change in the X-ray absorption spectrum when dust is added to the warm absorber. The thin straight line marks the intrinsic continuum, the fat line shows the best-fit warm-absorbed spectrum of NGC 4051. The dotted line corresponds to the same model, except for depleted metal abundances. The thin solid lines represent models including dust (and depleted abundances); the depletion factor of dust, relative to the standard Galactic-ISM mixture, is marked.

A third approach to  $Q$  is via the ionization-parameter sensitive emission-line ratio  $[\text{OII}]\lambda 3727/[\text{OIII}]\lambda 5007$  (e.g. Schulz & Komossa 1993), and using this method we find  $Q \simeq (1.7 - 3.4) \times 10^{52} \text{ s}^{-1}$ .

An additional EUV component may also explain the observational trend that broad emission lines and observed continuum seem to vary independently in NGC 4051 (e.g. Peterson et al. 1985, Rosenblatt et al. 1992), as expected if the observed optical-UV continuum variability is not fully representative of the EUV regime.

## 4 NGC 3227

NGC 3227 is a Seyfert 1.5 galaxy at a redshift of  $z=0.003$ . Although studied in many spectral regions, most attention has focussed on the optical wavelength range. NGC 3227 has been the target of several high spectral and spatial resolution studies and BLR mapping campaigns. Ptak et al. (1994) found evidence for a warm absorber in an *ASCA* observation.

### 4.1 Spectral analysis

For a single powerlaw description of the soft X-ray spectrum we obtain a very flat spectrum ( $\Gamma_x \simeq -1.2$ ), and strong systematic residuals remain. A powerlaw

with the canonical index of  $\Gamma_x = -1.9$ , modified by warm absorption, describes the data well. The alternative description, a soft excess on top of a powerlaw, results in an unrealistically flat slope with  $\Gamma_x \approx -1.1$ , in contradiction to higher-energy observations ( $\Gamma_x \simeq -1.9$ , George et al. 1990;  $\Gamma_x \simeq -1.6$ , Ptak et al. 1994).

#### 4.2 Temporal analysis

We find the source to vary by a factor of 3.5 in count rate during the 11 days of the pointed observation. The shortest resolved doubling timescale is 380 minutes. An analysis of the survey data reveals strong variability between survey observation and pointing (which are separated by  $\sim 3y$ ) with a maximum factor of  $\sim 15$  change in count rate. Unfortunately, the low number of photons accumulated during the survey does not allow a detailed spectral analysis.

Dividing the data in a hard and soft band, according to a photon energy of larger or less than 0.9 keV, we find correlated variability between both bands (Fig. 2), implying that no drastic spectral changes have taken place. The soft band includes most of the warm absorption features (which extend throughout this whole band; cf. Fig. 4) as well as the influence of the cold absorbing column, which consequently cannot be disentangled from that of the ionized material. Spectral fits to individual ‘orbits’ of the total observation show the ionization parameter  $U$  to be constant throughout the whole observation, independent of luminosity. (In this study, the cold and warm column densities were fixed to the values determined for the total observation.)

#### 4.3 Properties of the warm absorber

**A dusty absorber?** We find an ionization parameter of  $\log U \approx -1.0$  and a warm column density of  $\log N_w \approx 21.5$ . The cold column,  $N_H = 0.55 \times 10^{21} \text{ cm}^{-2}$  (corresponding to a reddening of  $A_v = 0^m.3$ , if accompanied by dust), is larger than the Galactic value ( $N_H^{Gal} \simeq 0.22 \times 10^{21} \text{ cm}^{-2}$ ), but not as large as indicated by line reddening. The narrow  $H\alpha/H\beta$  ratio measured by, e.g., Cohen (1983) implies an extinction of  $A_v \simeq 1.2$ . At another time, Mundell et al. (1995a) report a much higher value,  $A_v \simeq 4.5$ . The intrinsic Balmer line ratios are expected to be close to the recombination value under NLR conditions. A change in the  $H\alpha/H\beta$  ratio has then to be attributed to extinction by dust. However, dust *intrinsic* to the narrow line clouds is not expected to vary by factors of several within years, suggesting that the extinction is caused by an external absorber along the line of sight. If this dust is accompanied by an amount of gas as typically found in the Galactic interstellar medium, a large cold absorbing column of  $N_H \simeq 8.3 \times 10^{21} \text{ cm}^{-2}$  is expected to show up in the soft X-ray spectrum. (We note that the present X-ray observation and the optical observations by Mundell et al. (1995a) are not simultaneous, but they are only separated by  $6\frac{1}{2}$  months.) Such a large neutral column is *not* seen in soft X-rays. Dust mixed with the warm gas could supply the reddening without implying a corresponding cold column.

Fitting a sequence of (Galactic-ISM-like) dusty absorbers provides an excellent description of the soft X-ray spectrum, with  $\log U \approx -0.25$  and  $\log N_w \approx 21.8$ . The cold column is still slightly larger than the Galactic value, consistent with Mundell et al. (1995b), who find evidence for HI absorption towards the continuum-nucleus of NGC 3227.

Another possibility to explain the comparatively low cold column observed in X-rays is that we see scattered light originating from an extended component outside the nucleus. However, in that case the X-ray emission should not be that rapidly variable (e.g. Ptak et al. 1994; our Sect. 4.1). An alternative that cannot be excluded, due to the non-simultaneity of the observations, is that the material responsible for the reddening may have appeared only after the X-ray observation. In this scenario, it may not be associated with the warm absorber at all, but consist of thick blobs of dusty cold material crossing the line of sight. Since this is a possibility, we will include the dust-free warm absorber description of the data in the following discussion.

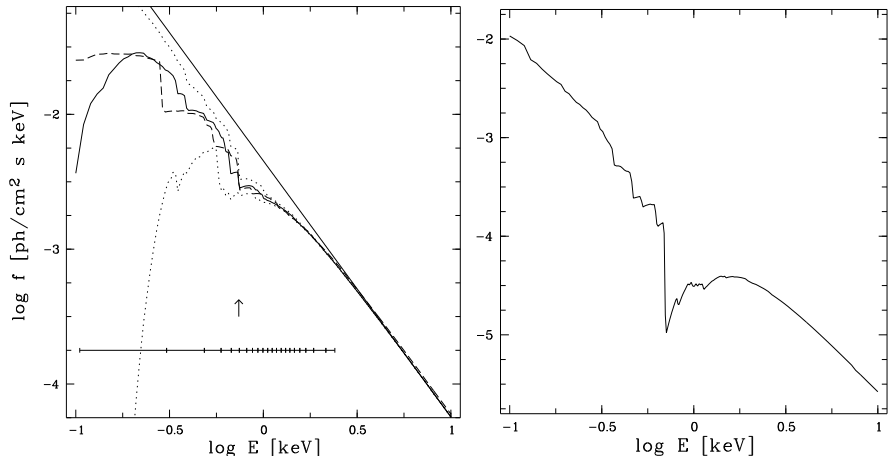


**Fig. 4.** Left: Warm-absorbed X-ray spectrum of NGC 3227 (solid line: dust-free, dashed: dusty model) between 0.1 and 10 keV, corrected for cold absorption. The straight line corresponds to the unabsorbed powerlaw. The dotted lines show the change in the absorption structure for a factor of 2 (upper curve) and a factor of  $\frac{1}{2}$  change in luminosity, and consequently in  $U$ . The two curves were shifted to match the normalization of the best-fit model, to allow a better comparison. The horizontal line at the bottom brackets the *ROSAT* sensitivity range, the vertical bars indicate the bin sizes in energy that were used in the spectral fitting. The arrow marks the position of the OVII edge. Right: Warm-absorbed X-ray spectrum of Mrk 1298.

**Density and Location** (i) For the dust-free best fit ( $\log U \simeq -1.0$ ), the density-scaled distance of the warm absorber is  $r \simeq 10^{16} \text{ cm} \times (n_{9.5})^{-0.5}$ , which compares to the typical BLR radius of  $r \simeq 17 \text{ ld} = 4 \times 10^{16} \text{ cm}$ , as determined from reverberation mapping (Salamanca et al. 1994, Winge et al. 1995). (ii) For the dusty warm absorber, the gas density has to be less than about  $10^7 \text{ cm}^{-3}$ , i.e.  $r \geq 9 \times 10^{16} \text{ cm} \times (n_7)^{-0.5}$ , to ensure dust survival. Constant ionization parameter throughout the observed low-state in flux (Sect. 4.2) further implies  $n \lesssim 2 \times 10^6 \text{ cm}^{-3}$ ; or even  $n \lesssim 2.5 \times 10^4 \text{ cm}^{-3}$ , based on the assumption of constant  $U$  during the total observation (less certain, due to time gaps in the data), and still using  $t_{\text{rec}}$  as an estimate. The ionized material has to be located at least between BLR and NLR, or even in the outer parts of the NLR, to extinct a non-negligible part of the NLR.

**Thermal stability** The thermal stability of the warm material is addressed in Fig. 5. Between the low-temperature ( $T \sim 10^4 \text{ K}$ ) and high-temperature ( $T \sim 10^{7-8} \text{ K}$ ) branch of the equilibrium curve, there is an intermediate region of multi-valued behavior of  $T$  in dependence of  $U/T$ , i.e. pressure (e.g., Guilbert et al. 1983; their Fig. 1). It is this regime, where the warm absorber is expected to be located, with its temperature typically found to lie around  $T \sim 10^5 \text{ K}$ . The detailed shape of the equilibrium curve in this regime depends strongly on the shape of the ionizing continuum, and properties of the gas, e.g. metal abundances. An analysis by Reynolds & Fabian (1995) placed the warm absorber in MCG-6-30-15 in a small stable regime within this intermediate region (its position is marked by an arrow in Fig. 5). The ionized material in NGC 3227 is characterized by a comparatively low ionization parameter. Its location in the  $T$  versus  $U/T$  diagram is shown for the models that provide a successful description of the X-ray spectrum. The shape of the equilibrium curve is clearly modified for the model including dust and correspondingly depleted metal abundances.

The locations of the warm absorbers in other objects of the present study are also plotted. They are found to lie all around the intermediate stable region. Interesting behavior is shown by the warm material in two observations of NGC 4051. A detailed assessment of the thermal stability of ionized absorbers is still difficult due to the strong influence of several parameters on the shape of the equilibrium curves.

**Line emission** From a sample of objects chosen to asses whether one of the known emission-line regions in active galaxies can be identified with the warm absorber, NGC 3227 represents the low-ionization end of the known warm absorbers. It also exhibits broad wings in  $\text{H}\alpha$  that do not follow continuum variations (Salamanca et al. 1994), indicative of a higher than usual ionized component, that may be identified with the warm absorber. (i) Dust-free warm absorber: The absorber-intrinsic luminosity in  $\text{H}\beta$  is only about 1/30 of the broad observed  $\text{H}\beta$  emission (Rosenblatt et al. 1994; de-reddened with  $A_v=0.9$ ). The scaled optical lines are weak, e.g.,  $[\text{FeX}]_{\text{wa}}/\text{H}\beta_{\text{obs}} \approx 0.03$ . The strongest line in the ultraviolet is  $\text{CIV}\lambda 1549$ , with  $\text{CIV}_{\text{wa}}/\text{H}\beta_{\text{obs}} \approx 6$ . A comparison of the expected line strengths with a typical BLR spectrum is shown in Fig. 6. (ii) In

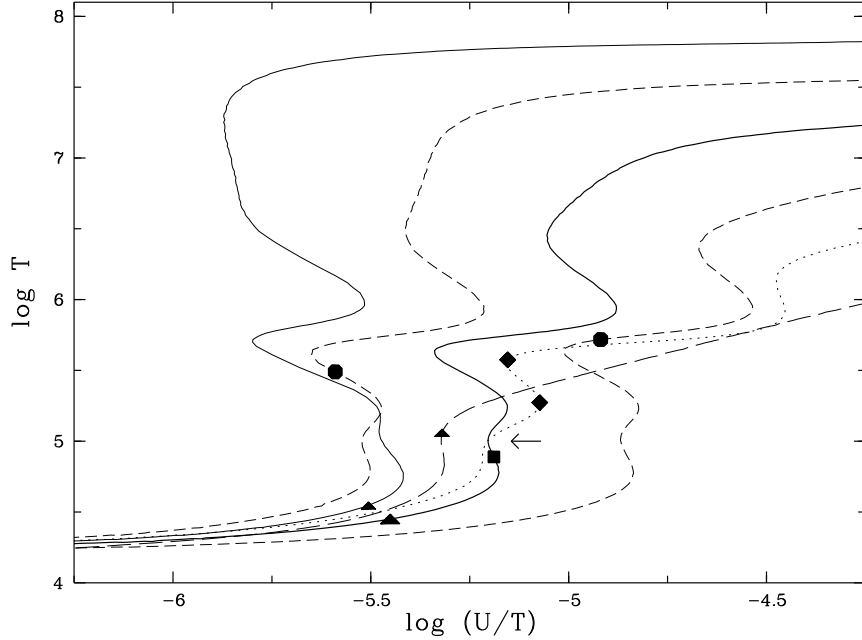


**Fig. 5.** Equilibrium gas temperature  $T$  versus  $U/T$  and locations of warm absorbers. The equilibrium curves are shown for different ionizing continua and gas properties, and the positions of the warm absorbers discussed in the present study are marked. The solid lines correspond to SEDs with (i)  $\Gamma_x = -1.6$  (left) and (ii)  $\Gamma_x = -1.9$  (right), and  $\alpha_{uv-x} = -1.4$ ; long-dashed: the same continuum as (ii), but gas of depleted metal abundances and with dust; short-dashed: ionizing continua employed for the NLSy1 galaxies RX J1239 (left,  $\alpha_{uv-x} = -0.75$ ) and RX J1225 ( $\alpha_{uv-x} = -1.9$ ); dotted: observed SED of NGC 4051 with  $\Gamma_x = -2.3$ . The symbols mark the positions that we derive for the warm absorbers from X-ray spectral fits; triangles: NGC 3227 (for the dusty and dust-free absorber model); square: Mrk 1298; lozenges: NGC 4051, Nov. 1991 observation (lower symbol) and Nov. 1993 observation; arrow pointed to solid line: MCG-6-30-15 (Reynolds & Fabian 1995); circles: RX J1239 (left) and RX J1225.

case of dust mixed with the ionized material, the overall emissivity is reduced and no strong emission lines are predicted.

**UV absorption lines** A comparison of UV absorption lines and X-ray absorption properties of active galaxies was performed by Ulrich (1988). Her analysis of an IUE spectrum of NGC 3227 in the range 2000 – 3200 Å revealed the presence of MgIIλ2798 absorption with an equivalent width of  $\log W_\lambda/\lambda \simeq -2.8$ . The X-ray warm absorber in NGC 3227 is of comparatively low ionization parameter. Nevertheless, the column density in MgII is very low, with  $\log W_\lambda/\lambda \simeq -5.7$  (and considerably lower for the dusty model). Predictions of UV absorption lines that

arise from the ionized material are made for the more highly ionized species, e.g.  $\log W_\lambda/\lambda \simeq -2.9$  ( $-3.0$ ) for CIV $\lambda 1549$ , and  $\log W_\lambda/\lambda \simeq -3.0$  ( $-3.1$ ) for NV $\lambda 1240$  (for  $b = 60$  km/s). The values in brackets refer to the warm absorber model that includes dust.

## 5 Mrk 1298

Mrk 1298 (PG 1126-041) is a luminous Seyfert 1 galaxy at a redshift of  $z = 0.06$ . The optical spectrum exhibits strong FeII emission. The presence of a warm absorber in the X-ray spectrum was found by Wang et al. (1996).

### 5.1 Spectral analysis

Again, the deviations of the X-ray spectrum from a single powerlaw fit are strong ( $\chi^2_{\text{red}} = 4.3$ ) with a rather steep slope of index  $\Gamma_x \simeq -2.6$ . Among various spectral models compared with the data (including those consisting of a soft excess on top of a powerlaw), only the warm absorber model provides a successful description. Due to the rather low number of detected photons, the underlying powerlaw index is not well constrained and was fixed to the canonical value of  $\Gamma_x = -1.9$ .

### 5.2 Properties of the warm absorber

We find an ionization parameter of  $\log U \simeq -0.3$  and a warm column density of  $\log N_w \simeq 22.2$ . The absorber-intrinsic line emission turns out to be negligible, with  $L_{\text{H}\beta}^{\text{wa}} = 1/740 L_{\text{H}\beta}^{\text{obs}}$ , except for OVI $\lambda 1035_{\text{wa}}/\text{H}\beta_{\text{obs}} = 0.4$ . Wang et al. (1996) mention the existence of strong UV absorption lines in an IUE spectrum. Here we find indeed rather large column densities in C $^{3+}$  and N $^{4+}$ , corresponding to an equivalent width for, e.g., CIV of  $\log W_\lambda/\lambda \simeq -2.9$  (for  $b = 60$  km/s).

**Table 1.** Properties of the warm absorbers in the three Seyfert galaxies. For comparison results from a single powerlaw fit are shown.

name	date of obs.	warm absorber					single powerlaw		
		$N_{\text{H}}^{(1)}$	$\Gamma_x$	$\log U$	$\log N_w$	$\chi^2_{\text{red}}$	$N_{\text{H}}^{(1)}$	$\Gamma_x$	$\chi^2_{\text{red}}$
NGC 4051	Nov. 1991	0.13 <sup>(2)</sup>	-2.2	0.2	22.5	1.1	0.18	-2.8	2.8
	Nov. 1993	0.13	-2.3	0.4	22.7	1.1	0.17	-2.9	3.8
NGC 3227	May 1993	0.55	-1.9	-1.0	21.5	0.8	0.38	-1.2	1.7
		0.55	-1.9	-0.3	21.8	0.7 <sup>(3)</sup>			
Mrk 1298	June 1992	0.44 <sup>(2)</sup>	-1.9	-0.3	22.2	0.9	0.44 <sup>(2)</sup>	-2.6	4.3

<sup>(1)</sup> in  $10^{21}$  cm $^{-2}$  <sup>(2)</sup> Galactic value <sup>(3)</sup> model including dust

## 6 Narrow Line Seyfert 1 Galaxies

Several extremely X-ray soft Seyferts have been found recently that belong to the class of NLSy1 galaxies (e.g. Puchnarewicz et al. 1992), which are characterized by narrow Balmer lines, and often strong FeII emission (e.g. Goodrich 1989). One interpretation of the X-ray spectral steepness is the dominance of the hot tail of emission from an accretion disk (e.g. Boller et al. 1996). Another one, which will be explored below, is the presence of a warm absorber.

In fact, a natural consequence of the observation of absorption *edges* in the X-ray spectra of Seyfert galaxies, is to also expect objects with deeper absorption, with mainly the ‘down-turning’ part of the absorption-complex being visible in the *ROSAT* sensitivity region. Good such candidates are ultrasoft AGN, and some are studied in the following.

### 6.1 RX J1239.3+2431 and RX J1225.7+2055

The 2 NLSy1 galaxies were discovered in *ROSAT* survey observations and exhibit very steep X-ray spectra (formally  $\Gamma_x \simeq -3.7$  and  $-4.3$ ; Greiner et al. 1996) and there is slight evidence for a spectral upturn within the *ROSAT* band. A description of the X-ray spectra in terms of warm absorption is found to be successful, albeit not unique due to the poor photon statistics of the survey data. We find  $\log U \approx 0.8$  ( $\log \tilde{U} \approx 0.4$ ) and  $\log N_w \approx 23.2$  for RX J1225, and  $\log U \approx -0.1$  ( $\log \tilde{U} \approx 0.2$ ) and  $\log N_w \approx 22.8$  for RX J1239.

The absorber-intrinsic H $\beta$  emission is rather large and corresponds to about 1/10 and 1/7 of the observed  $L_{H\beta}$  for RX J1225 and RX J1239, respectively. Scaling the predicted [FeXIV] $\lambda 5303$  emission of the warm material in order not to conflict with the observed upper limit ( $\lesssim 0.15$ ) constrains the covering factor of the gas to  $\lesssim 1/6$  in RX J1239 and is consistent with 1 in RX J1225. Given the high discovery rate of supersoft AGN among X-ray selected ones (e.g. Greiner et al. 1996), the covering factors indeed have to be high to account for this fact. For both objects, several strong ultraviolet emission lines are predicted, e.g. HeII $\lambda 1640_{\text{wa}}/H\beta_{\text{obs}} \simeq 1.3$ , FeXXI $\lambda 1345_{\text{wa}}/H\beta_{\text{obs}} \simeq 1.1$  in RX J1225. The corresponding emission-line spectrum is illustrated in Fig. 6 assuming the maximal covering consistent with the data.

### 6.2 RX J0119.6-2821

RX J0119 (1E 0117.2-2837) was discovered as an X-ray source by *Einstein* and is at a redshift of  $z=0.347$  (Stocke et al. 1991). It is serendipitously located in one of the *ROSAT* PSPC pointings.

The X-ray spectrum is very steep. When described by a single powerlaw continuum with Galactic cold column, the photon index is  $\Gamma_x \simeq -3.6$  ( $-4.3$ , if  $N_H$  is a free parameter). The overall quality of the fit is good ( $\chi^2_{\text{red}} \simeq 1$ ), but there are slight systematic residuals around the location of absorption edges. Again, a successful alternative description is a warm-absorbed flat powerlaw of

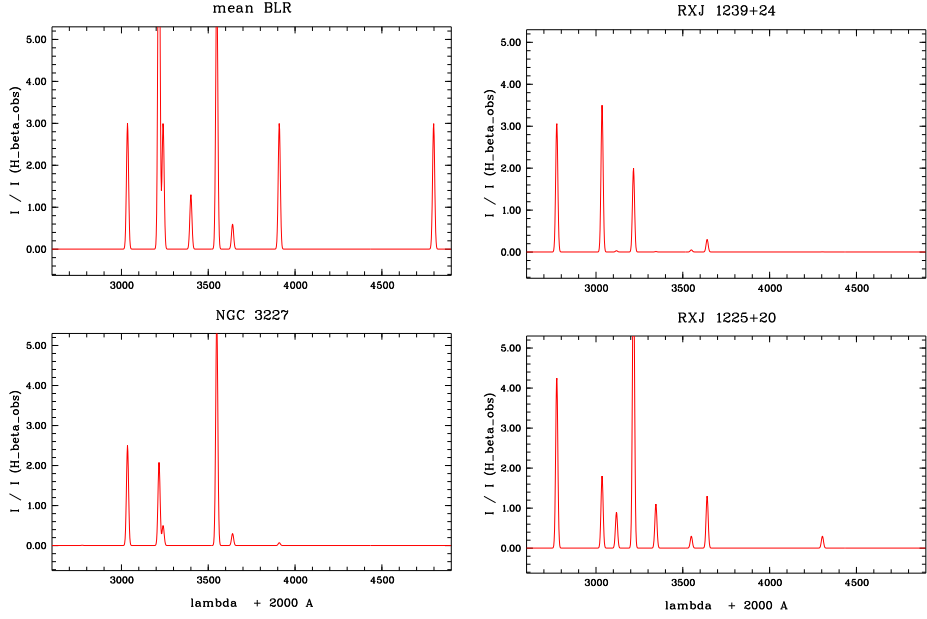


**Fig. 6.** Emission line spectra in the range  $600 - 2900 \text{ \AA}$  predicted to arise from the warm material in individual objects compared to a mean BLR spectrum, to give an impression on the strengths of these lines and allow a judgement of the detectability. The y-axis gives the intensity of the absorber-intrinsic emission lines relative to the observed broad  $\text{H}\beta$  emission for the individual objects.

canonical index. We find a very large column density  $N_w$  in this case, and the contribution of emission and reflection is no longer negligible; there is also some contribution to  $\text{Fe K}\alpha$ . For the pure absorption model, the best-fit values for ionization parameter and warm column density are  $\log U \simeq 0.8$ ,  $\log N_w \simeq 23.6$  ( $N_H$  is consistent with the Galactic value), with  $\chi^2_{\text{red}} = 0.74$ . Including the contribution of emission and reflection for 50% covering of the warm material gives  $\log N_w \simeq 23.8$  ( $\chi^2_{\text{red}} = 0.65$ ).

Several strong EUV emission lines arise from the warm material. Some of these are:  $\text{FeXXI}\lambda 2304/\text{H}\beta = 10$ ,  $\text{HeII}\lambda 1640/\text{H}\beta = 16$ ,  $\text{FeXXI}\lambda 1354/\text{H}\beta = 37$ ,  $\text{FeXVIII}\lambda 975/\text{H}\beta = 16$ ,  $\text{NeVIII}\lambda 774/\text{H}\beta = 9$ , and, just outside the IUE sensitivity range for the given  $z$ ,  $\text{FeXXII}\lambda 846/\text{H}\beta = 113$ . No absorption from CIV and NV is expected to show up. Both elements are more highly ionized.

### 6.3 RX J0134.3-4258

This object exhibits an ultrasoft spectrum in the *ROSAT* survey data (Dec. 1990; formally  $\Gamma_x \simeq -4.4$ ). Interestingly, the spectrum has changed to flat in a

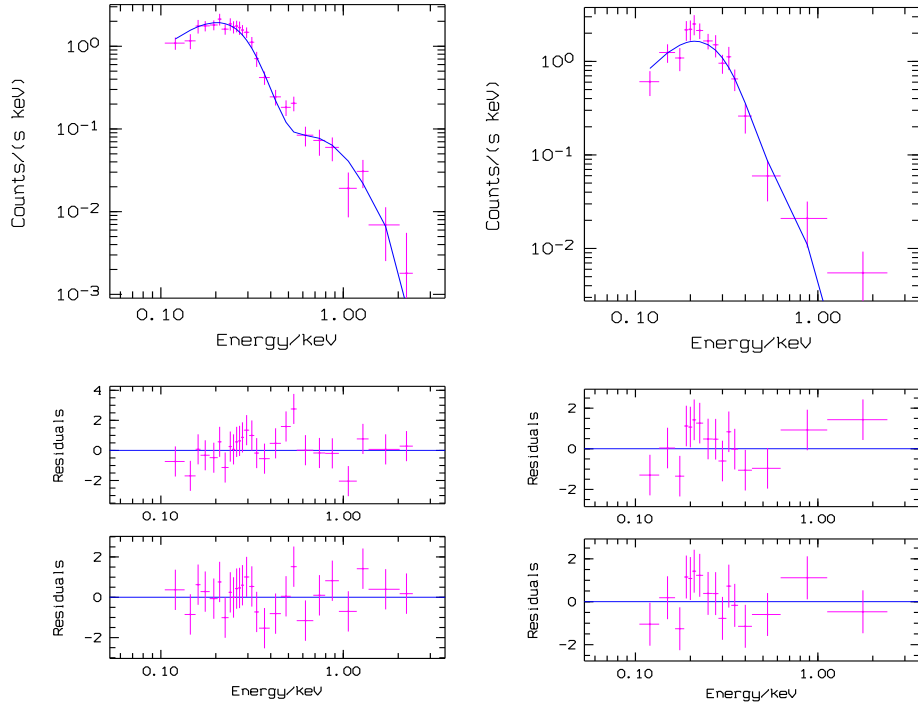


**Fig. 7.** Left: Powerlaw fit to the X-ray spectrum of RX J0119 (upper panel) and residuals, compared to the residuals for the warm absorber fit (lower panel; note the different scale in the ordinate). Right: Accretion disk fit to the ‘outburst’ observation of NGC 5905 (upper panel) and residuals, compared to residuals for the warm absorber fit (lower panel).

subsequent pointing (Dec. 1992;  $\Gamma_x \simeq -2.2$ ). This kind of spectral variability is naturally predicted within the framework of warm absorbers, making the object a very good candidate.

We find that a warm-absorbed, intrinsically flat powerlaw can indeed describe the survey observation. Due to the low number of available photons, a range of possible combinations of  $U$  and  $N_w$  explains the data with comparable success. A large column density  $N_w$  (of the order  $10^{23} \text{ cm}^{-2}$ ) is needed to account for the ultrasoft observed spectrum. The most suggestive scenario within the framework of warm absorbers is a change in the *ionization state* of ionized material along the line of sight, caused by *varying irradiation* by a central ionizing source. In the simplest case, lower intrinsic luminosity would be expected, in order to cause the deeper observed absorption in 1990. However, the source is somewhat brighter in the survey observation (Fig. 8). Some variability seems to be usual, though, and the count rate changes by about a factor of 2 during the pointed observation. If

one wishes to keep this scenario, one has to assume that the ionization state of the absorber still reflects a preceding (unobserved) low-state in intrinsic flux. Alternatively, gas heated by the central continuum source may have *crossed the line of sight*, producing the steep survey spectrum, and has (nearly) disappeared in the 1992 observation.

It is interesting to note, that the optical spectrum of RX J0134 rises to the blue (Grupe 1996), and a soft excess on top of a powerlaw continuum may represent an alternative explanation of the data.

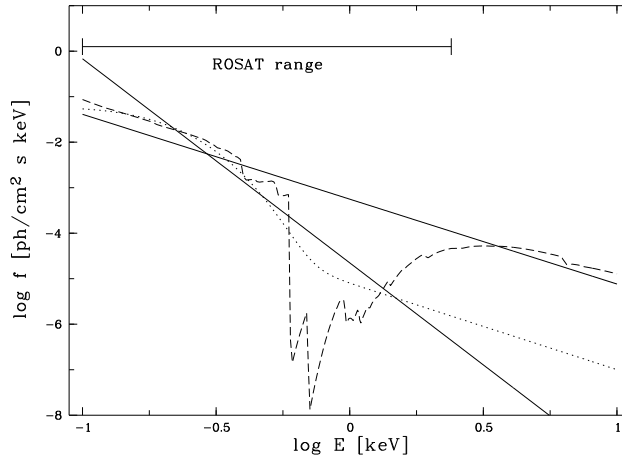


**Fig. 8.** Comparison of different X-ray spectral fits to the *ROSAT* survey observation of RX J0134 (thick lines) and the pointed observation (thin solid line). Thick solid: single powerlaw with  $\Gamma_x = -4.4$ ; dashed: warm-absorbed flat powerlaw; dotted: powerlaw plus soft excess, parameterized as a black body. All models are corrected for cold absorption.

**Table 2.** Comparison of different spectral fits to the NLSy1 galaxies: (i) single powerlaw (pl), (ii) accretion disk after Shakura & Sunyaev (1973), and (iii) warm absorber.  $\Gamma_x$  was fixed to  $-1.9$  in (ii) and (iii), except for RX J0134, where  $\Gamma_x = -2.2$  (see text).

name	powerlaw <sup>(1)</sup>			acc. disk + pl <sup>(2)</sup>			warm absorber <sup>(2)</sup>		
	$N_{\text{H}}^{(3)}$	$\Gamma_x$	$\chi_{\text{red}}^2$	$M_{\text{BH}}^{(4)}$	$\frac{\dot{M}}{\dot{M}_{\text{edd}}}$	$\chi_{\text{red}}^2$	$\log U$	$\log N_{\text{w}}$	$\chi_{\text{red}}^2$
RX J1239.3+2431	0.32	-4.3	1.2	0.7	0.4	1.4	-0.1	22.8	1.0
RX J1225.7+2055	0.29	-3.7	1.9	1.0	0.5	2.1	0.8	23.2	1.8
RX J0119.6-2821	0.30	-4.3	0.8	0.6	0.6	0.7	0.8	23.6	0.7
RX J0134.3-4258 <sup>(5)</sup>	0.16	-4.4	0.5	11.4	0.1	0.6	0.5	23.1	0.6

<sup>(1)</sup>  $N_{\text{H}}$  free, if  $> N_{\text{H}}^{\text{Gal}}$  <sup>(2)</sup>  $N_{\text{H}}$  fixed to  $N_{\text{H}}^{\text{Gal}}$  <sup>(3)</sup> in  $10^{21} \text{ cm}^{-2}$  <sup>(4)</sup> in  $10^4 M_{\odot}$  <sup>(5)</sup> survey obs.

#### 6.4 Warm absorbers in *all* NLSy1 galaxies ?

There are some NLSy1 galaxies in which the warm absorber is clearly present and causes indeed at least most of the observed spectral steepness, as e.g. in NGC 4051. Mrk 1298 is another example. It exhibits all characteristics of NLSy1s, except that its observed FWHM of H $\beta$ , 2200 km/s, just escapes the criterion of Goodrich (1989). One of the comfortable properties of the warm-absorber interpretation is the presence of enough photons to account for the strong observed FeII emission in NLSy1s, due to the intrinsically flat powerlaw. It does not immediately explain the occasionally observed trend of *stronger* FeII in objects with *steeper* X-ray spectra, but it is interesting to note that Wang et al. (1996) find a trend for stronger FeII to preferentially occur in objects whose X-ray spectra show the presence of absorption edges.

There are, however, other objects where neither a flat powerlaw with soft excess nor a warm absorber can account for most of the spectral steepness, although the presence of such a component cannot be excluded, as we have verified for **1Zw1** and **PHL 1092**.

In any model – warm absorber, accretion-produced soft excess, or intrinsically steep powerlaw spectrum – it is still difficult to elegantly account for all observational trends; as are, besides strong FeII, the tendency for narrower FWHM of broad H $\beta$  for steeper X-ray spectra (e.g. Boller et al., their Fig. 8), and a slight anti-correlation of optical and soft X-ray spectral index (Grupe 1996). Progress is reported in Wandel (1996). Critical comments on the distinction between different models concerning photoionization aspects are given in Komossa & Greiner (1995).

To conclude, a warm absorber was shown to successfully reproduce the X-ray spectra of several NLSy1s and thus may well mimic the presence of a soft excess. High quality spectra are needed to distinguish between several possible models. In fact, although the warm absorber dominates the X-ray spectrum of the well-studied galaxy NGC 4051, an additional soft excess is present in flux high-states, and the underlying powerlaw is steeper than usual (Sect. 3.1). This hints to the complexity of NLSy1 spectra, with probably more than one mechanism at work to cause the X-ray spectral steepness.

### 7 The X-ray outburst in the HII galaxy NGC 5905

NGC 5905 underwent an X-ray ‘outburst’ during the *ROSAT* survey observation, with a factor  $\sim 100$  change in count rate. The high-state spectrum is simultaneously very soft and luminous (Bade, Komossa & Dahlem 1996). Its classification (based on an optical pre-outburst spectrum) is HII type. Comparable variability was found in two further objects (IC3599; Brandt et al. 1995, Grupe et al. 1995a, WPVS007; Grupe et al. 1995b). The outburst mechanism is still unclear; tidal disruption of a star by a central black hole has been proposed. In the following, we comment on this and other possibilities and then discuss whether the X-ray outburst spectrum of NGC 5905 can be explained in terms of warm absorption.

**SN in dense medium** The possibility of ‘buried’ supernovae (SN) in *dense* molecular gas was studied by Shull (1980) and Wheeler et al. (1980). In this scenario, X-ray emission originates from the shock, produced by the expansion of the SN ejecta into the ambient interstellar gas of high density. Since high luminosities can be reached this way, and the evolutionary time is considerably speeded up, an SN in a dense medium may be an explanation for the observed X-ray outburst in NGC 5905.

Assuming the observed  $L_x \approx 3 \times 10^{42}$  erg/s of NGC 5905 to be the peak luminosity, results in a density of the ambient medium of  $n_4 \simeq \times 10^6 \text{ cm}^{-3}$  (using the estimates from Shull (1980) and Wheeler et al. (1980), and assuming line cooling to dominate with a cooling function of  $\Lambda \propto T^{-0.6}$ ), but is inconsistent with the observed softness of the spectrum: The expected temperature is  $T \approx 10^8$  K, compared to observed one of  $T \approx 10^6$  K. Additionally, fine-tuning in the column density of the surrounding medium would be needed in order to prevent the SNR from being completely self-absorbed.

**Tidal disruption of a star** The idea of tidal disruption of stars by a supermassive black hole (SMBH) was originally studied as a possibility to fuel AGN, but dismissed. Later, Rees (1988, 1990) proposed to use individual such events as tracers of SMBHs in nearby galaxies. The debris of the disrupted star is accreted by the BH. This produces a flare, lasting of the order of months, with the peak luminosity in the EUV or soft X-ray spectral region.

The luminosity emitted if the BH is accreting at its Eddington luminosity can be estimated by  $L_{\text{edd}} \simeq 1.3 \times 10^{38} M/M_{\odot}$  erg/s. In case of NGC 5905, a BH mass of  $\sim 10^4 M_{\odot}$  would be necessary to produce the observed  $L_x$  (assuming it to be observed near its peak value). In order to reach this luminosity, a mass supply of about  $1/2000 M_{\odot}/\text{y}$  would be sufficient, assuming  $\eta=0.1$ .

**Accretion disk instabilities** If a massive BH exists in NGC 5905, it has to usually accrete with low accretion rate or radiate with low efficiency, to account for the comparatively low X-ray luminosity of NGC 5905 in ‘quiescence’. An accretion disk instability may provide an alternative explanation for the observed X-ray outburst. Thermally unstable slim accretion disks were studied by Honma et al. (1991), who find the disk to exhibit burst-like oscillations for the case of the standard  $\alpha$  viscosity description and for certain values of accretion rate.

Using the estimate for the duration of the high-luminosity state (Honma et al. 1991; their eq. 4.8), and assuming the duration of the outburst to be less than 5 months (the time difference between the first two observations of NGC 5905), a central black hole of mass in the range  $\sim 10^4 - 10^5 M_{\odot}$  can account for the observations. The burst-like oscillations are found by Honma et al. only for certain values of the initial accretion rate. A detailed quantitative comparison with the observed outburst in NGC 5905 is difficult, since the behavior of the disk is quite model dependent, and further detailed modeling would be needed.

**Warm-absorbed hidden Seyfert** Since all previous scenarios are either unlikely (SN in dense medium) or require some sort of fine-tuning, we finally asses the possibility of a warm-absorbed Seyfert nucleus. In this scenario, a hidden

Seyfert resides within the HII-type galaxy, that is slightly variable and usually hidden by a cold column of absorbing gas. The nucleus gets ‘visible’ during its flux high-states by ionizing the originally cold column of surrounding gas that becomes a *warm* absorber, thereby also accounting for the softness of the outburst spectrum.

We find that the survey spectrum can be well described by warm absorption with  $\log U \simeq 0.0$  and  $\log N_w \simeq 22.8$ . A source-intrinsic change in luminosity by a factor of less than 10 is needed to change the absorption to complete within the *ROSAT* band. Variability of such order is not unusual in low-luminosity AGN; e.g., NGC 4051 has been found to be variable by about a factor of 30 within 2 years (Sect. 3.2). Since there is no evidence for Seyfert activity in the optical spectrum, the nucleus must be hidden. Mixing dust with the warm gas results in an optical extinction of  $A_v \approx 34^m$  (assuming a Galactic gas-to-dust ratio) and would hide the Seyfert nucleus completely. The spectrum in the low-state – with a luminosity of  $L_x \approx 4 \times 10^{40}$  erg/s and a shape that can be described by a powerlaw with  $\Gamma_x \approx 2.4$  – can be accounted for by the usual X-ray emission of the host galaxy (e.g. Fabbiano 1989). However, dust with Galactic ISM properties internal to the warm gas was shown to strongly influence the X-ray absorption structure. An acceptable fit to the X-ray spectrum can only be achieved by tuning the dust properties and the dust depletion factor.

There are several ways to decide upon different scenarios: A hidden Seyfert nucleus should reveal its presence by a permanent hard X-ray spectral component, as observable e.g. with *ASCA*. One may also expect repeated flaring activity in the accretion-disk and warm-absorber scenario, and a *ROSAT* HRI monitoring (PI: N. Bade) is underway.

*Acknowledgement:* The *ROSAT* project is supported by the German Bundesministerium für Bildung, Wissenschaft, Forschung und Technologie (BMBF/DARA) and the Max-Planck-Society. We thank Gary Ferland for providing *Cloudy*.

## References

Bade N., Komossa S., Dahlem M., 1996, A&A 309, L35  
 Boller T., Brandt W.N., Fink H.H., 1996, A&A 305, 53  
 Brandt W.N., Pounds K.A., Fink H.H., 1995, MNRAS 273, L47  
 Brandt W.N., Fabian, A.C., Pounds K.A., 1996, MNRAS 278, 326  
 Cappi M., Mihara T., Matsuoka M., Hayashida K., Weaver K.A., Otani C., 1996, ApJ 458, 149  
 Cohen R.D., 1983, ApJ 273, 489  
 Fabbiano G., 1989, ARA&A 27, 87  
 Fabian A.C., 1996, MPE Report 263, H.U. Zimmermann, J. Trümper, H. Yorke (eds.), 403  
 Ferland G.J., 1993, University of Kentucky, Physics Department, Internal Report  
 Fiore F., Elvis M., Mathur S., Wilkes B.J., McDowell J.C., 1993, ApJ 415, 129  
 George I.M., Nandra K., Fabian, A.C., 1990, MNRAS 242, 28p  
 Goodrich R.W., 1989, ApJ 342, 224

Greiner J., Danner R., Bade N., Richter G.A., Kroll P., Komossa S., 1996, A&A 310, 384

Grevesse N., Anders E., 1989, in Cosmic Abundances of Matter, C.J. Waddington (ed.), AIP 183

Grupe D., Beuermann K., Mannheim K., Bade N., Thomas H.-C., de Martino D., Schwope A., 1995a, A&A 299, L5

Grupe D., Beuermann K., Mannheim K., Thomas H.-C., Fink H.H., de Martino D., 1995b, A&A 300, L21

Grupe D., 1996, Ph.D. thesis, Universität Göttingen

Guilbert P.W., Fabian A.C., McCray R., 1983, ApJ 266, 466

Halpern J.P., 1984, ApJ 281, 90

Hamann F., Zuo L., Tytler D., 1995, ApJ 444, L69

Honma F., Matsumoto R., Kato S., 1991, PASJ 43, 147

Komossa S., Greiner J., 1995, AG abstract series 11, 217

Komossa S., Fink H., 1996, AG abstract series 12, 227

Komossa S., Fink H., 1997, A&A, in press

Kriss G.A., Krolik J.H., Otani C., Espey B.R., Turner T.J., Kii T., Tsvetanov Z., Takahashi T., Davidson A.F., Tashiro H., Zheng W., Murakami S., Petre R., Mihara T., 1996, ApJ 467, 629

Krolik J.H., Kallman T.R., 1984, ApJ 286, 366

Krolik J.H., Kriss G.A., 1995, ApJ 447, 512

Laor A., Draine B.T., 1993, ApJ 402, 441

Mathur S., Wilkes B., Elvis M., Fiore F., 1994, ApJ 434, 493

McHardy I.M., Green A.R., Done C., Puchnarewicz E.M., Mason K.O., Branduardi-Raymont G., Jones M.H., 1995, MNRAS 273, 549

Mihara T., Matsuoka M., Mushotzky R., Kunieda H., Otani C., Miyamoto S., Yamauchi M., 1994, PASJ 46, L137

Mundell C., Holloway A.J., Pedlar A., Meaburn J., Kukula M.J., Axon D.J., 1995a, MNRAS 275, 67

Mundell C., Pedlar A., Axon D.J., Meaburn J., Unger S.W., 1995b, MNRAS 277, 641

Murray N., Chiang J., Grossman S.A., Voit G.M., 1995, ApJ 451, 498

Nandra K., Pounds K.A., 1992, Nature 359, 215

Netzer H., 1990, in Saas-Fee Lecture Notes 20, T.J.-L. Courvoisier and M. Mayor (eds.)

Netzer H., 1993, ApJ 411, 594

Netzer H., Laor A., 1993, ApJ 404, L51

Otani C., Kii T., Reynolds C. S., et al., 1996, PASJ 48, 211

Peterson B.M., Crenshaw D.M., Meyers K.A., 1985, ApJ 298, 283

Pounds K.A., Nandra K., Fink H.H., Makino F., 1994, MNRAS 267, 193

Ptak A., Yaqoob T., Serlemitsos P.J., Mushotzky R., Otani C., 1994, ApJL 436, L31

Puchnarewicz E.M., Mason K.O., Cordova F.A., Kartje J., Branduardi-Raymont G., Mittaz P.D., Murdin P.G., Allington-Smith J., 1992, MNRAS 256, 589

Rees M.J., 1988, Nature 333, 523

Rees M.J., 1990, Science 247, 817

Reynolds C.S., Fabian, A.C., 1995, MNRAS 273, 1167

Rosenblatt E.I., Malkan M.A., Sargent W.L.W., Readhead A.C.S., 1992, ApJS 81, 59

Rosenblatt E.I., Malkan M.A., Sargent W.L.W., Readhead A.C.S., 1994, ApJS 93, 73

Salamanca I., Alloin D., Baribaud T., et al., 1994, A&A 282, 742

Schartel N., Komossa S., Brinkmann W., Fink, H.H., Trümper, J., Wamsteker, W., 1997, A&A, in press

Schulz H., Komossa S., 1993, A&A 278, 29  
 Shakura N.I., Sunyaev R.A., 1973, A&A 24,337  
 Shull J.M., 1980, ApJ 237, 769  
 Shull J.M., Van Steenberg M., 1982, ApJS 48, 95 & ApJS 49, 351  
 Spitzer L., 1978, Physical Processes in the Interstellar Medium  
 Stocke J.T., Morris S.L., Gioia I.M., Maccacaro T., Schild R., Wolter A., Fleming T.A.,  
     Henry J.P., 1991, ApJS 76, 813  
 Turner T.J., Nandra K., George I.M., Fabian A.C., Pounds K.A., 1993, ApJ 419, 127  
 Ulrich M.-H., 1988, MNRAS 230, 121  
 Ulrich-Demoulin M.-H., Molendi S., 1996, ApJ 457, 77  
 Wandel A., 1996, in X-Ray Imaging and Spectroscopy of Cosmic Hot Plasmas, Ab-  
     stracts, 73  
 Wang T., Brinkmann W., Bergeron J., 1996, A&A 309, 81  
 Ward M., Elvis M., Fabbiano G., Carleton N. P., Willner S. P., Lawrence A., 1987,  
     ApJ 315, 74  
 Weaver K.A., Yaqoob T., Holt S.S., Mushotzky R.F., Matsuoka M., Yamauchi M.,  
     1994, ApJ 436, L27  
 Wheeler J.C., Mazurek T.J., Sivaramakrishnan A., 1980, ApJ 237, 781  
 Witt H.J., Czerny B., Zycki P.T., 1996, MNRAS, in press  
 Winge C., Peterson B., Horne K., Pogge R.W., Pastoriza M., Storchi-Bergmann T.,  
     1995, ApJ 445, 680  
 Zimmermann H.U., Becker W., Belloni T., Döbereiner S., Izzo C., Kahabka P., Schwen-  
     tke O., 1994, MPE report 257